Unraveling the Aggregation Propensity of Human Insulin C-Peptide

Paraskevi L. Tsiolaki,[1] Nikolaos N. Louros,[1] Aikaterini A. Zompra,[2] Stavros J. Hamodrakas,[1] Vassiliki A. Iconomidou[1]

[1]*Department of Cell Biology and Biophysics, Faculty of Biology, University of Athens, Panepistimiopolis, Athens, 15701, Greece*

[2]*Department of Pharmacy, University of Patras, Patras, 26504, Greece*

Received 15 February 2016; revised 19 May 2016; accepted 31 May 2016
Published online 3 June 2016 in Wiley Online Library (wileyonlinelibrary.com). DOI 10.1002/bip.22882

ABSTRACT:

Over the last 20 years, proinsulin C-peptide emerged as an important player in various biological events. Much time and effort has been spent in exploring all functional features of C-peptide and recording its implications in Diabetes mellitus. Only a few studies, though, have addressed C-peptide oligomerization and link this procedure with Diabetes. The aim of our work was to examine the aggregation propensity of C-peptide, utilizing Transmission Electron Microscopy, Congo Red staining, ATR-FTIR, and X-ray fiber diffraction at a 10 mg ml^{-1} concentration. Our experimental work clearly shows that C-peptide self-assembles into amyloid-like fibrils and therefore, the aggregation propensity of C-peptide is a characteristic novel feature that should be related to physiological and also pathological conditions. © *2016 Wiley Periodicals, Inc. Biopolymers (Pept Sci) 108: 1–8, 2017.*

Keywords: insulin biosynthesis; proinsulin C-peptide; diabetes mellitus; amyloids; amyloidogenic peptides

This article was originally published online as an accepted preprint. The "Published Online" date corresponds to the preprint version. You can request a copy of any preprints from the past two calendar years by emailing the Biopolymers editorial office at biopolymers@wiley.com.

INTRODUCTION

Structural studies of peptides and proteins during the last few years revealed an increasing number of the so-called "amyloidogenic proteins". A large number of human proteins, chemically and structurally divergent, may undergo general or partial refolding and may subsequently self-assemble into amyloid fibrils, causing degenerative diseases such as Alzheimer's disease, Parkinson's disease, prion diseases, or Diabetes type 2.[1,2] Amyloid diseases are characterized by the presence of amyloid deposits composed mainly of one amyloidogenic protein. The 2014 Amyloid Fibril Protein Nomenclature List includes all well characterized amyloidogenic proteins to-date.[3]

C-peptide (Figure 1b) was for several years a forgotten parameter in insulin studies, but today has been proven to be a bioactive peptide.[4] Proinsulin (Figure 1a), the truncated product of pre-proinsulin, consists of 86 amino acids, where C-peptide is the 31 amino acid linker (Figure 1a, blue color) between insulin A chain (Figure 1a, deep red color) and insulin B chain (Figure 1a, green color).[5–7] During normal insulin biosynthesis in pancreatic β-cells, proinsulin is able to fold quickly into its correct three-dimensional structure, by forming three disulfide bridges, two interchain bonds and one intrachain bond (Figure 1a, yellow dashed lines).[5] Following this folding process, proinsulin is transferred in clathrin coated immature secretory vesicles to the Golgi complex.[8] Granule maturation is completed within 2 h after synthesis; at pH near acidic conditions (~5.0−5.5), where prohormone serine endoproteases, convertase PC2 and convertase PC1/3 act in combination, and the clathrin coating is removed.[9–11]

Additional Supporting Information may be found in the online version of this article.

Correspondence to: Vassiliki A. Iconomidou; Department of Cell Biology and Biophysics, Faculty of Biology, University of Athens, Panepistimiopolis, Athens 157 01, Greece; e-mail: veconom@biol.uoa.gr

Contract grant sponsor: University of Athens
Contract grant sponsor: European Union (European Regional Development Fund – ERDF), Greek national funds through the Operational Program "Competitiveness and Entrepreneurship" of the National Strategic Reference Framework (NSRF) (General Secretariat for Research and Technology of the Greek Ministry of Education and Religious Affairs, Culture and Sports)
Contract grant number: 11SYN-1-1230

© 2016 Wiley Periodicals, Inc.

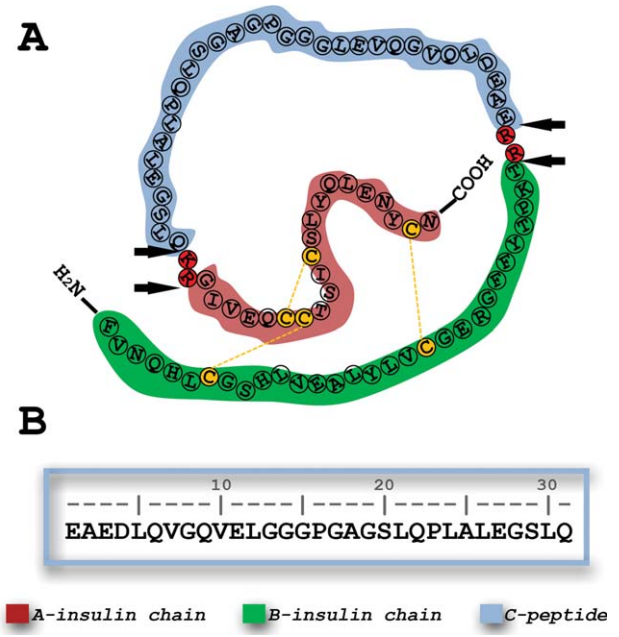

FIGURE 1 Schematic representation of human proinsulin and amino acid sequence of proinsulin C-peptide. A: A graphical respresentation of human proinsulin; insulin A chain and B chain are shown in red and green respectively and proinsulin C-peptide, the connecting peptide between A and B chains, is shown in blue. Cysteines are shown in yellow and disulfide bridges are marked with yellow dashed lines. Arrows indicate sites of proteolytic activity into β-cell granules (See Introduction). B: The amino acid composition of the 31 amino acid human proinsulin C-peptide (Uniprot AC: P01308).

The generation of native insulin and free C-peptide is accomplished by carboxypeptidase-E (CPE), which eliminates C-terminal basic amino acids exposed by the convertases (Figure 1a, black arrows).[12] This mechanism results in the retention of both insulin and C-peptide in the mature storage granules in equal amounts.[13] However, mature β-cell granules also contain other peptides, including islet amyloid polypeptide (IAPP or amylin), chromogranins, other minor components and even small amounts of proinsulin or proinsulin intermediates and proIAPP.[8,13,14] The final exocytotic release of insulin from the β-cell storage vesicles into the blood is an energy-dependent process, as a response to the sugar level in blood.[15] Both insulin and C-peptide are released together into the circulation in equimolar amounts.[13]

Studies concerning proinsulin C-peptide function are constantly enriched.[16] It is absolutely crucial in insulin biosynthesis, since C-peptide is the essential join between A and B chains. C-peptide participation in proinsulin structure fulfills the important biological role of facilitating the formation of the correct secondary and tertiary structure of insulin and preventing insulin aggregation.[7,17] Recent studies have reported several molecular interactions of C-peptide,[18–20] cell signaling events,[21] and pivotal effects in diabetic patients.[20]

Apart from mature insulin, whose three dimensional structure was determined by X-ray crystallography, proinsulin and C-peptide adopt unordered structures in solution, as NMR spectroscopy confirmed[22,23] and, interestingly, free insulin (chains A and B) displays similar overall conformation to that of proinsulin.[24] Although most researchers agree that the C-peptide structure is unordered under physiological conditions, a few studies reveal that C-peptide is not a random coil, but rather contains detectable ordered structure both when free or attached to insulin in proinsulin[25]; the N-terminal part (*1*-EAEDLQVGQVE−*11*) may adopt an α-helical conformation at high concentrations of trifluoroethanol (TFE)[26] and Molecular Dynamics simulations suggest turn-like motifs in the middle part and the C-terminal of C-peptide.[27]

It has been shown that C-peptide segments are related to its function: The N-terminal part of the proinsulin C-peptide acts as a chaperon and contributes to proper insulin folding, by preventing insulin aggregation.[28–31] The C-terminal region contains an interaction epitope for binding to a G-protein coupled receptor,[32] while the C-terminal pentapeptide *27*-EGSLQ−*31* specifically, simulates the way the full-length C-peptide binds to a cell surface.[33] The middle segment (residues 12 − 26) of proinsulin C-peptide, with a high turn propensity, is considered to be flexible due to its sequence composition and it is suggested to mediate C-peptide – membrane interactions at low pH.[27,34]

C-peptide interferes with Diabetes mellitus; patients with type 2 Diabetes (T2D) produce reduced insulin, in contrast to patients with type 1 Diabetes (T1D), which have lost all of their capacity to secrete insulin.[15,35] Since insulin and C-peptide are co-secreted in equimolar amounts, C-peptide release was first used as an independent "biomarker" (or diagnostic tool) of insulin secretory rate, *in vivo*, in diabetic patients.[36,37] Moreover, in type 1 and type 2 Diabetes, where pancreatic β-cells are under stress and consequently misfunction, the incomplete proinsulin cleavage results in elevated circulating proinsulin levels.[38] Furthermore, C-peptide treatment was reported to be beneficial for diabetic subjects in combination with daily insulin injections. The most well-known therapeutic possibilities of C-peptide are gathered together in a recent excellent review article.[39]

Several studies highlight the therapeutic potential of C-peptide in diabetes, only a few studies, though, unveil the formation of C-peptide oligomers[31,40] and the accumulation of C-peptide in the vessel walls in early atherogenesis, in diabetic patients.[41] Taking all the above studies into consideration, in the present study, we decided to test the propensity of C-peptide to self-assemble into amyloid fibrils, *in vitro*. The C-peptide was found to self-assemble into amyloid-like fibrils at a concentration of 10 mg ml^{-1} in distilled water and,

therefore, here we discuss this novel important finding in relation to Diabetes and to physiological conditions.

MATERIALS AND METHODS

Peptide Synthesis

The 31 amino acid C-peptide (Figure 1b) was synthesized by GeneCust© Europe, Luxembourg. The purity of the synthesized peptide was 96.8% (free N- and C-terminals).

Preparation of Amyloid-Like Fibrils

The synthesized peptide was dissolved in distilled water (pH 5.5), at a concentration of 10 mg ml^{-1}, and after one week incubation at ambient (room) temperatures, C-peptide forms amyloid-like fibril-containing gels. Oriented fibers, suitable for X-ray diffraction, were obtained from suspensions of C-peptide mature amyloid fibrils, as described below.

X-Ray Diffraction

A droplet (~10 μl) of mature fibril suspension was placed between two quartz capillaries covered with wax, spaced ~1.5 mm apart and mounted horizontally on a glass substrate, as collinearly as possible, to obtain an oriented fiber. The X-ray diffraction pattern from this fiber was collected, using a SuperNova-Agilent Technologies X-ray generator equipped with a 135-mm ATLAS CCD detector and a 4-circle kappa goniometer, at the Institute of Biology, Medicinal Chemistry and Biotechnology, National Hellenic Research Foundation (CuK_α high intensity X-ray micro-focus source, $\lambda = 1.5418$ Å), operated at 50 kV, 0.8 mA. The specimen-to-film distance was set at 52 mm and the exposure time was set to 400 s. The X-ray patterns, initially were viewed using the program CrysAlisPro[42] and consequently measured with the aid of the program iMosFLM.[43] Indexing (h, k, l, d_{obs}, d_{calc}) of C-peptide was done utilizing DICVOL06.[44]

Negative Staining and Transmission Electron Microscopy

For negative staining, droplets (~3 − 5 μl) of C-peptide mature fibril suspensions were applied to glow-discharged 400-mesh carbon-coated copper grids for 60 s. The grids were stained with a droplet (5 μl) of 2% (w/v) aqueous uranyl acetate for 60 s. Excess stain was removed by blotting with a filter paper. The grids were air-dried. The fibril-containing grids were examined with a Morgagni^{TM} 268 transmission electron microscope, operated at 80 kV. Digital acquisitions were performed with an 11Mpixel side-mounted Morada CCD camera (Soft Imaging System, Muenster, Germany).

Attenuated Total Reflectance Fourier-Transform Infrared Spectroscopy (ATR FTIR) and Post-Run Computations of the Spectra

A 10-μl droplet of C-peptide mature fibril suspension was cast on a front-coated Au mirror and left to dry slowly at ambient conditions to form a thin film. Infrared spectra were obtained from these films at a resolution of 4 cm^{-1}, utilizing an IR microscope (IRScope II by Bruker Optics) equipped with a Ge attenuated total reflectance (ATR) objective lens (20x) and attached to a Fourier-transform infrared (FTIR) spectrometer (Equinox 55, by Bruker Optics). Internal reflection spectroscopy has several advantages compared with the more common KBr dispersion technique.[45] The choice of ATR was dictated by the need to exclude any possible spectroscopic and chemical interactions between the sample and the dispersing medium. Having a penetration depth ca. 1–2 μm (1000 cm^{-1}, Ge), ATR is free of saturation effects, which may be present in the transmission spectra of thicker samples. Moreover, the use of a microscope facilitates the acquisition of data from small samples. Ten 32-scan spectra were collected from each sample and averaged to improve the S/N ratio. The spectra are shown in the absorption mode after correction for the wavelength dependence of the penetration depth (pd ~ λ). Absorption band maxima were determined from the minima in the second derivative of the corresponding spectra. Derivatives were computed analytically using routines of the Bruker OPUS/OS2 software and included smoothing by the Savitzky–Golay algorithm over a ± 8 cm^{-1} range, around each data point. Smoothing over narrower ranges resulted in a deterioration of the S/N ratio and did not increase the number of minima that could be determined with confidence.

Congo Red Staining and Polarized Light Microscopy

C-peptide mature fibril suspensions were applied to glass slides and stained with a 10 m*M* Congo Red (Sigma) solution in PBS (phosphate-buffered saline, pH 7.4) for ~30 min. Then, they were washed several times with 90% ethanol and left to dry approximately for 10 min. The samples were observed under bright field illumination and between crossed polars, using a Leica MZ75 polarizing stereomicroscope, equipped with a JVC GC-X3E camera.

Congo Red Spectroscopic Assay

Totally, 10 μl droplets of C-peptide (10 mg ml^{-1} final concentration) were used to record spectra between 400 and 700 nm at room temperature for a period of 7 days, following previous protocols.[46] Congo Red stain was prepared as described above. Absorption spectra were collected by a BIO-RAD SmartSpec^{TM} 3000 Spectrophotometer (170-2501), utilizing polystyrene disposable cuvettes (1 cm optical length). A 10 m*M* Congo Red spectrum was used as a reference (see Supporting Information data).

RESULTS

Transmission electron microscopy and negative staining clearly demonstrate that the C-peptide folds and self-assembles, after 1 week of incubation in distilled water at pH 5.5, forming a gel which mainly contains fibrils, which display the basic characteristics of amyloid fibrils: they appear to be straight and unbranched supercoils of indeterminate length and of different diameters. Each supercoil consists of protofibrils, with a diameter of ~50 Å (Figure 2, single arrow). The simplest such supercoils are helices (Figure 2, double arrows) and have a thickness of ca. 90 − 120 Å, whereas more complex supercoils, of various diameters, are frequently seen (Figure 2, triple arrows). Moreover, frequently, C-peptide amyloid-like fibrils tend to coalesce laterally to form bundles (Figure 2,

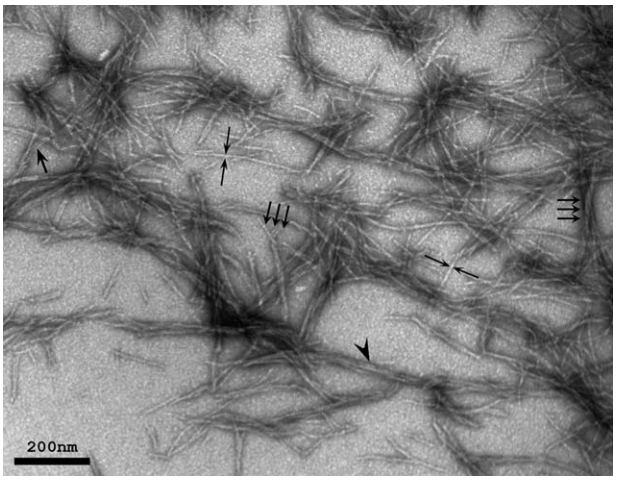

FIGURE 2 Transmission electron microscopy image of negatively stained proinsulin C-peptide amyloid-like fibrils. Proinsulin C-peptide self-assembles forming unbranched supercoils of undetermined length and different diameters (multiple arrows). Multi-stranded bundles were also observed for C-peptide (arrowhead). An individual protofibril is indicated with a single black arrow (ca. 50 Å in diameter). Bar is 200 nm.

arrowhead). Such polymorphism is common in amyloid fibril containing samples.[47,48]

C-peptide fibrils show strong affinity for the Congo red dye and exhibit the characteristic red–green birefringence of amyloid fibrils, when viewed under crossed polars (Figure 3). Along with polarizing microscopy findings, a Congo Red spectrophotometric approach elucidates a spectral shift from 500 nm to 540 nm, indicating that Congo Red binding occurs as the concentration of C-peptide amyloid fibrils increases. Additional electron microscopy micrographs were obtained after 0, 3, and 7 days of incubation, respectively, which confirm the spectroscopic analysis. The absorption spectra of Congo Red solution and Congo Red – C-peptide mixture are shown in Supporting Information Figure S1.

The X-ray diffraction patterns of oriented fibres produced from the amyloid-like fibril suspensions of the C-peptide, indicate a powder-like pattern of a polycrystalline material (Figure 4). The intense meridional reflection at 4.68 Å is attributed to the distance between hydrogen-bonded β-strands within β-sheet. The strong, but diffuse, reflection corresponding to a 8.7 Å periodicity may be attributed to the side chain packing distance between adjacent β-sheets. The above reflections are characteristic of the "cross-β" conformation,[49] and are observed for several amyloid-like fibrils,[50] in which the β-strands are perpendicular to the fiber axis and the sheets are packed parallel to the fiber axis (Figure 4). A list of the reflections observed in the X-ray pattern (Figure 4) is given in Table I. A full explanation of the polycrystalline diffraction pattern is given in the legend of Table I, with a table of the *d*-spacings of the diffraction rings and a proposed unit cell for the C-peptide fiber/"crystallites".

As shown in Figure 5 the ATR FTIR spectrum of C-peptide fibrils, cast as a thin-hydrated film, shows a prominent band at 1625 cm^{-1} in the amide I region and the two amide II bands at 1552 cm^{-1} and 1527 cm^{-1}, which are definitely due to β-sheet conformation.[51] The amide I, high wavenumber component at 1697 cm^{-1} is an indication that the β-sheets are antiparallel.[52–54] Other ATR FTIR bands and their tentative assignments are shown in Table II. [54–56] Thus, the results from ATR FTIR spectroscopy strongly support the evidence from X-ray diffraction.

DISCUSSION

The objective of this study was to investigate the amyloidogenic propensity of proinsulin C-peptide *in vitro*. For this

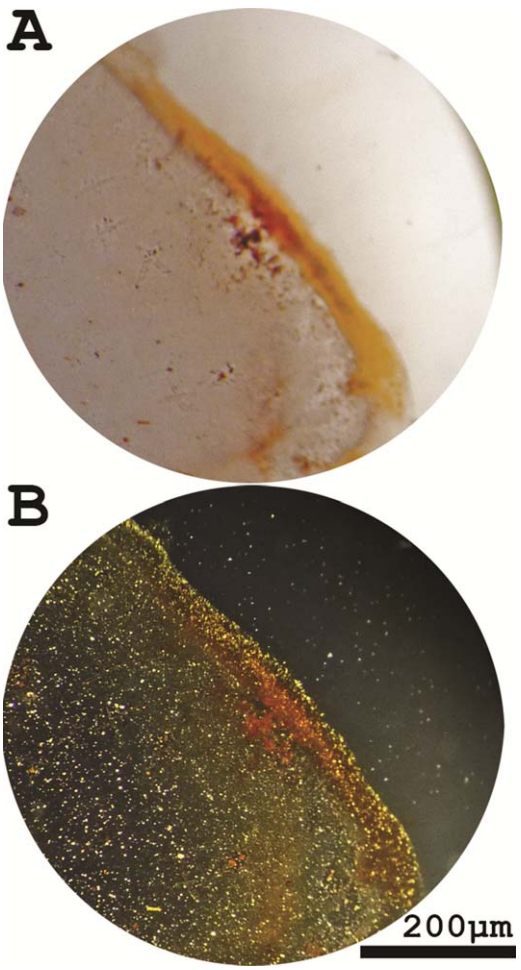

FIGURE 3 Proinsulin C-peptide Congo Red staining. A 10 mg ml^{-1} solution of C-peptide was incubated in distilled water (at ambient temperatures, pH 5.5), for ~7 days to produce mature amyloid-like fibrils. A hydrated thin film of C-peptide shows red−green birefringence in polarized light (b) after Congo red staining (a). (Bar 200 μm).

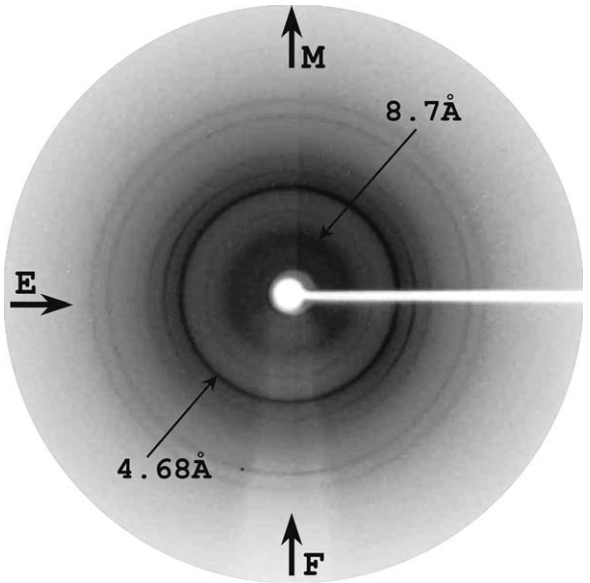

FIGURE 4 X-ray diffraction pattern from aligned C-peptide mature amyloid-like fibrils. Oriented fibers, derived from Cpeptide amyloid-like fibrils, show a powder-like X-ray diffraction pattern of a polycrystalline material. Reflections with spacings at 4.68 Å and 8.7 Å, respectively, are indicated with arrows. Table I contains a list of d-spacings of the diffraction rings and a possible unit cell for the C-peptide fiber/crystallite is proposed.

reason, the 31 amino acid C-peptide was chemically synthesized and dissolved in distilled water. The results reported above suggest that C-peptide intrinsically exhibits the tendency to self-assemble into amyloid fibrils (Figure 2) and, further, fulfills all three characteristic, structural, and tinctorial features of amyloids (Figures 3−5).

Table I Spacings (d_{obs}) of the Reflections That Were Observed in the Polycrystalline X-Ray Diffraction Pattern, Taken From a Fiber of the C-Peptide Amyloid-Like Fibrils

h	K	l	d_{obs} (Å)	d_{calc}(Å)
0	3	0	8.70	8.69
4	2	0	7.60	7.60
3	2	2	6.00	5.99
8	0	0	4.68	4.67
3	6	0	4.12	4.11
2	7	0	3.67	3.67
9	6	0	3.01	3.00
10	6	1	2.80	2.80

Indexing (h, k, l, d_{obs}, d_{calc}) was done, utilizing DICVOL06 [44], a software for the automatic indexing of powder diffraction patterns by the successive dichotomy method, based on an orthorhombic unit cell, with unit cell parameters: $a = 37.50 \pm 0.02$ Å, $b = 26.18 \pm 0.01$ Å, $c = 16.10 \pm 0.01$ Å, alpha = 90°, beta = 90°, gamma = 90°. This unit cell has a volume, Vol = 15431.2 Å^3 and it is estimated to contain 4 molecules of C-peptide.

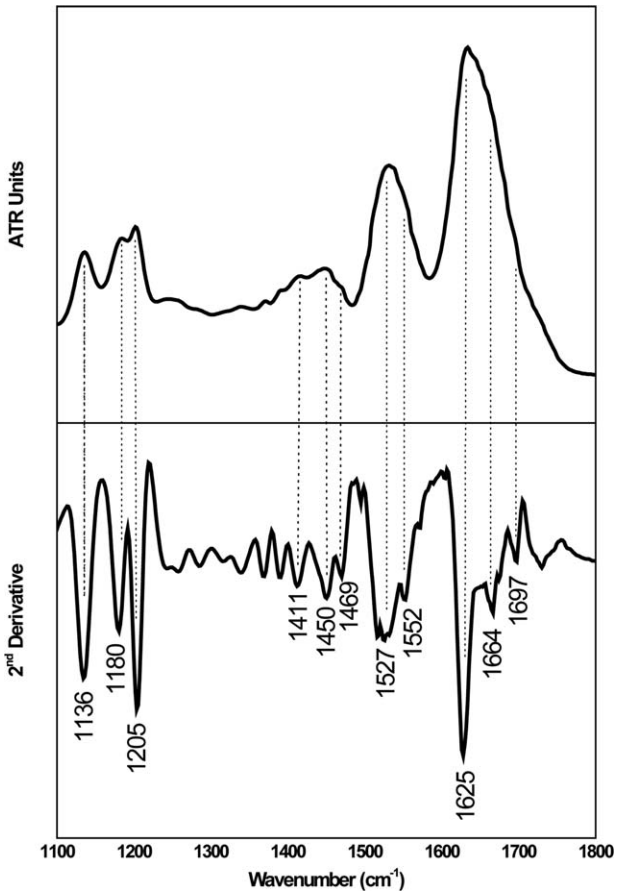

FIGURE 5 ATR FT-IR (1100–1800 cm^{-1}) spectrum of proinsulin C-peptide. Suspensions of mature amyloid fibrils derived from the C-peptide were cast on a flat stainless-steel plate (SpectRIM, Tienta Sciences, Inc. Indianapolis, USA) and left to air-dry slowly, at ambient conditions, in order to form a hydrated, thin film. Observed bands from the ATR FT-IR spectrum obtained from this film and their tentative assignments are given in Table II. A second derivative spectrum is also included.

Table II Bands Observed in the ATR FTIR (1100 − 1800 cm^{-1}) Spectrum Produced From a Hydrated Film of the Amyloidogenic C-Peptide After Self-Assembly, and Their Tentative Assignments (Figure 5)

Band (cm^{-1})	Assignment
1136	TFA
1180	TFA
1205	TFA
1411	Pro[55]
1450	CH_2[56], Pro[55]
1469	CH_2[56]
1527	Amide II (β-sheet)
1552	Amide II (β-sheet)
1625	Amide I (β-sheet)
1664	TFA
1697	Amide I (antiparallel β-sheet)

These novel features of proinsulin C-peptide should be carefully taken into account, since early studies of C-peptide self-aggregation stated clearly that C-peptide on its own does not give rise to amyloid fibrils.[57] Several peptides and proteins, which had not previously been associated with amyloidoses, (as C-peptide in our case), have been proven to form amyloid-like fibrils *in vitro*, indicating that amyloid formation may be an inherent ability of proteins under specific conditions.[1,2] Furthermore, *in vitro* studies using synthetic amyloidogenic proteins have been highly important for understanding the mechanisms by which proteins accumulate and subsequently may be involved in degenerative diseases.[58]

Aiming at a better understanding of C-peptide aggregation, it is worth mentioning that, in general, the control of the oligomeric states of a peptide is being driven by the relative concentration of the protein. *In vitro* assays of C-peptide utilized initial concentrations, ranging from 1mg ml^{-1} to 40 mg ml^{-1}.[17,31,57,59] Similar conditions are also commonly used at *in vitro* fibrillation assays of other "aggregation-prone" proteins and peptides.[60–62] Importantly, C-peptide levels at physiological conditions, such as fasting and postprandial conditions, are low.[63] However, the growing literature on Diabetes highlights that high concentration of C-peptide is observed in overweight individuals[64] and subjects with type 2 Diabetes,[65] because of the increase of C-peptide biological half-life.[38] At the same time, in atherogenesis, C-peptide was found to accumulate and deposit in the vessel walls of diabetic patients.[41]

As observed in our previous studies,[60,66] electron microscopy micrographs did not always show the presence of a polycrystalline material. However, several studies indicate structural similarities of diffracting features of protein fibrils and microcrystals.[67,68] Interestingly, *in vitro* assembly assays on a highly amyloidogenic peptide revealed that thin, single fibrils transform into lamellar nano-crystals.[60,69] Working systematically on elucidating amyloids at atomic level, Marshall and Serpell remark that "degree of order" is what really differentiates a crystal and a fibril-containing fiber.[70] In our case, C-peptide reflections appear as rings, indicating poor alignment of C-peptide constituent fibrils that lack higher molecular organization (Figure 4).

Further *in vitro* experiments on C-peptide detected a potent "amyloidogenic profile". C-peptide oligomers, observed by SDS-PAGE, indeed bind Thioflavin T and thus, researchers proposed a possible β-sheet conformation in an attempt to describe C-peptide affinity to the "amyloid specific" dye.[31,40] Moreover, to obtain structural clues on C-peptide, Lind et al. performed CD and ATR-IR spectroscopy on a mixture of C-peptide with SDS and in analogy to the results of our study, this publication was the first to mention that C-peptide oligomeric states are similar to other amyloidogenic peptides.[40]

Interestingly, using electrospray mass spectrometry Nerelius et al. extensively studied homo-interactions and aggregation of C-peptide fragments and revealed that N- and C-terminal segments, corresponding to C-peptide residues *1*-EAEDL−*5* and *27*-EGSLQ−*31* respectively, are prone to homo-oligomerize.[31,71] The use of our consensus secondary structure prediction algorithm SECSTR[72] suggests a possible α-helix for residues *1*-EAEDLQVGQV-*10* (at least two methods out of six) and also predicts a second shorter α-helix formed by residues *22*-QPLALE-*27* (at least two methods out of six) (Supporting Information Figure S2). SECSTR, though, suggests an alternative prediction for a β-strand for residues *6*-QVGQVE-11 (at least two methods out of six) and a weaker prediction for a β-strand for residues *21*-LQPL-*24*, overlapping the above α-helical predicted segments. Thus, these results imply that N- and C- terminals of the C-peptide have all the distinctive features of "chameleon" sequences[73] and therefore intrinsically exhibit the tendency to 'alter' their conformation depending on the environmental conditions. Accordingly, recent evolutionary studies of mammalian C-peptide sequences (~30 amino acid each), utilizing the PSIPRED prediction algorithm,[74] predict a strong β-strand propensity for residues *8*-GQVEL-*12* and propose that due to the conformation of this part, C-peptide may possibly adopt a hairpin-like structure.[75]

Another interesting issue to consider regarding the hidden amyloidogenic propensity of C-peptide is that homo-oligomerization is not connected with C-peptide chaperone-like effects on insulin.[71] Ordinarily, the formation of stable Zn^{2-} insulin hexamers into β-cell secretory granules, where C-peptide plays a critical role, prevents mature insulin from misfolding and consequently, ensures pancreatic β-cell integrity. Taking into account proinsulin particular features, such as this propensity to assemble in order to form Zn^{2-} coordinate hexamers,[5] Huang et al. performed Raman spectroscopy experiments on insulin fragments and suggested that the connecting peptide of proinsulin (35 amino acids), which corresponds to C-peptide (31 amino acids) including four dibasic residues (cleavage sites), decelerates the fibrillation procedure and, in other words, protects zinc-free insulin from misfolding.[76] Significantly though, both insulin and proinsulin (86 amino acids) form amyloid-like "structures" *in vitro*; mature insulin self-assembles at acidic conditions into amyloid fibrils which fulfill all amyloid criteria,[59,77,78] in contrast to proinsulin, which forms an amorphous β-sheet-rich precipitate (neutral pH) rather than typical amyloid fibrils.[76]

Biological effects, reviewed in the article [80], suggest that C-peptide may act as a parameter with a major contribution in metabolic "fine-tuning" of the tissues,[79] since it accomplishes an important role in the synthesis of insulin. According to our findings, previously undefined oligomeric forms in

atherogenesis of diabetic patients[41,65] or overweight individuals[64] should be reconsidered. A critical question regarding the amyloidogenicity of C-peptide should definitely be raised in Diabetes mellitus, and further, more targeted experiments should be done. This approach is reasonable because, in the vast majority of amyloidoses, two or more abnormal proteins accumulate simultaneously, forming amyloid co-deposits.[80,81]

To date, protein-based products are rapidly entering the pharmaceutical industry as successful drugs,[82] and therefore a better understanding on protein aggregation is needed.[83] Extensive studies shed light on several therapeutic aspects of C-peptide in Diabetes.[39,84] Since fibrillation of insulin has long complicated its use in the treatment of Diabetes, causing Insulin-derived amyloidosis at injection site (Iatrogenic amyloidosis),[78,85] aggregation propensity of C-peptide should also carefully be taken into account. Controlling C-peptide self-aggregation may allow an optimized design of a C-peptide-based treatment in type I Diabetes therapy, where preliminary clinical trials have indeed been promising.[86]

The authors thank our collaborator Dr. Evangelia D. Chrysina for excellent assistance with the X-ray experiments and the Institute of Biology, Medicinal Chemistry and Biotechnology at the National Hellenic Research Foundation for hospitality. They thank Dr. Georgios E. Baltatzis and Prof. Efstratios S. Patsouris for excellent assistance with Transmission Electron Microscopy experiments in the Department of Pathology, at the Medical School of the University of Athens. Finally, they would like to thank the handling editor and the reviewers of this manuscript for their very useful and constructive criticism.

REFERENCES

1. Chiti, F.; Dobson, C. M. Annu Rev Biochem 2006, 75, 333–366.
2. Uversky, V. N.; Fink, A. L. Biochim Biophys Acta 2004, 1698, 131–153.
3. Sipe, J. D.; Benson, M. D.; Buxbaum, J. N.; Ikeda, S.; Merlini, G.; Saraiva, M. J.; Westermark, P. Amyloid 2014, 21, 221–224.
4. Wahren, J.; Ekberg, K.; Jornvall, H. Diabetologia 2007, 50, 503–509.
5. Dodson, G.; Steiner, D. Curr Opin Struct Biol 1998, 8, 189–194.
6. Steiner, D. F.; Oyer, P. E. Proc Natl Acad Sci USA 1967, 57, 473–480.
7. Steiner, D. F. N Engl J Med 1969, 280, 1106–1113.
8. Steiner, D. F.; Bell, G. I.; Rubenstein, A. H.; Chan, S.J. Endocrinology; W.B. Saunders: Philadelphia, 2006; Chapter 48.
9. Seidah, N. G.; Chretien, M. Brain Res 1999, 848, 45–62.
10. Muller, L.; Lindberg, I. Prog Nucleic Acid Res Mol Biol 1999, 63, 69–108.
11. Zhou, A.; Webb, G.; Zhu, X.; Steiner, D. F. J Biol Chem 1999, 274, 20745–20748.
12. Fricker, L. D.; Evans, C. J.; Esch, F. S.; Herbert, E. Nature 1986, 323, 461–464.
13. Steiner, D. F.; Philipson, L. H. In Insulin Biosynthesis, Secretion, Structure, and Structure-Activity Relationships; De Groot, L. J., et al., Eds.; Endotext: South Dartmouth (MA), 2000.
14. Lukinius, A.; Wilander, E.; Westermark, G. T.; Engstrom, U.; Westermark, P. Diabetologia 1989, 32, 240–244.
15. Seino, S.; Bell, I. G. Pancreatic Beta Cell in Health and Disease. Springer: Japan, 2008.
16. Steiner, D. F. Exp Diabesity Res 2004, 5, 7–14.
17. Shafqat, J.; Melles, E.; Sigmundsson, K.; Johansson, B. L.; Ekberg, K.; Alvelius, G.; Henriksson, M.; Johansson, J.; Wahren, J.; Jornvall, H. Cell Mol Life Sci 2006, 63, 1805–1811.
18. Johansson, J.; Ekberg, K.; Shafqat, J.; Henriksson, M.; Chibalin, A.; Wahren, J.; Jornvall, H. Biochem Biophys Res Commun 2002, 295, 1035–1040.
19. Wahren, J.; Ekberg, K.; Shafqat, J.; Johansson, J.; Johansson, B. L.; Jörnvall, H. Biological Effects of C-Peptide and Proinsulin, 3rd ed.; Wiley: Chichester, 2004.
20. Landreh, M.; Jornvall, H. FEBS Lett 2015, 589, 415–418.
21. Hills, C. E.; Brunskill, N. J. Exp Diabetes Res 2008, 2008, 635158.
22. Munte, C. E.; Vilela, L.; Kalbitzer, H. R.; Garratt, R. C. FEBS J 2005, 272, 4284–4293.
23. Yang, Y.; Hua, Q. X.; Liu, J.; Shimizu, E. H.; Choquette, M. H.; Mackin, R. B.; Weiss, M. A. J Biol Chem 2010, 285, 7847–7851.
24. Weiss, M. A.; Frank, B. H.; Khait, I.; Pekar, A.; Heiney, R.; Shoelson, S. E.; Neuringer, L. J Biochemistry 1990, 29, 8389–8401.
25. Brems, D. N.; Brown, P. L.; Heckenlaible, L. A.; Frank, B. H. Biochemistry 1990, 29, 9289–9293.
26. Henriksson, M.; Shafqat, J.; Liepinsh, E.; Tally, M.; Wahren, J.; Jornvall, H.; Johansson, J. Cell Mol Life Sci 2000, 57, 337–342.
27. Mares-Guia, T. R.; Maigret, B.; Martins, N. F.; Maia, A. L.; Vilela, L.; Ramos, C. H.; Neto, L. J.; Juliano, M. A.; dos Mares-Guia, M. L.; Santoro, M. M. J Mol Graph Model 2006, 25, 532–542.
28. Chen, L. M.; Yang, X. W.; Tang, J. G. J Biochem 2002, 131, 855–859.
29. Qiao, Z. S.; Min, C. Y.; Hua, Q. X.; Weiss, M. A.; Feng, Y. M. J Biol Chem 2003, 278, 17800–17809.
30. Min, C. Y.; Qiao, Z. S.; Feng, Y. M. Eur J Biochem 2004, 271, 1737–1747.
31. Jornvall, H.; Lindahl, E.; Astorga-Wells, J.; Lind, J.; Holmlund, A.; Melles, E.; Alvelius, G.; Nerelius, C.; Maler, L.; Johansson, J. Biochem Biophys Res Commun 2010, 391, 1561–1566.
32. Yosten, G. L.; Kolar, G. R.; Redlinger, L. J.; Samson, W. K. J Endocrinol 2013, 218, B1–B8.
33. Rigler, R.; Pramanik, A.; Jonasson, P.; Kratz, G.; Jansson, O. T.; Nygren, P.; Stahl, S.; Ekberg, K.; Johansson, B.; Uhlen, S.; Uhlen, M.; Jornvall, H.; Wahren, J. Proc Natl Acad Sci USA 1999, 96, 13318–13323.
34. Unnerstale, S.; Maler, L. J Biophys 2012, 2012, 185907.
35. Kahn, S. E. Diabetologia 2003, 46, 3–19.
36. Rubenstein, A. H.; Melani, F.; Pilkis, S.; Steiner, D. F. Postgrad Med J 1969, 45, 476–481.
37. Polonsky, K. S.; Licinio-Paixao, J.; Given, B. D.; Pugh, W.; Rue, P.; Galloway, J.; Karrison, T.; Frank, B. J Clin Invest 1986, 77, 98–105.
38. Rhodes, C. J.; Alarcon, C. Diabetes 1994, 43, 511–517.
39. Wahren, J.; Larsson, C. Diabetes Res Clin Pract 2015, 107, 309–319.
40. Lind, J.; Lindahl, E.; Peralvarez-Marin, A.; Holmlund, A.; Jornvall, H.; Maler, L. FEBS J 2010, 277, 3759–3768.
41. Marx, N.; Walcher, D.; Raichle, C.; Aleksic, M.; Bach, H.; Grub, M.; Hombach, V.; Libby, P.; Zieske, A.; Homma, S.; Strong, J. Arterioscler Thromb Vasc Biol 2004, 24, 540–545.

42. CrysAlis^{PRO}, 2014. Agilent Technologies, p. Software system, Agilent Technologies UK Ltd, Oxford, UK, pp. Software system.
43. Leslie, A. G. W.; Powell, H. R. 2007. Processing diffraction data with mosflm. Springer Netherlands, Dordrecht, The Netherlands.
44. Boultif, A.; Louër, D. J Appl Crystallography 2004, 37, 724–731.
45. de Jongh, H. H.; Goormaghtigh, E.; Ruysschaert, J. M. Anal Biochem 1996, 242, 95–103.
46. Nilsson, M. R. Methods 2004, 34, 151–160.
47. Kreplak, L.; Aebi, U. Adv Protein Chem 2006, 73, 217–233.
48. Meinhardt, J.; Sachse, C.; Hortschansky, P.; Grigorieff, N.; Fandrich, M. J Mol Biol 2009, 386, 869–877.
49. Geddes, A. J.; Parker, K. D.; Atkins, E. D.; Beighton, E. J Mol Biol 1968, 32, 343–358.
50. Sunde, M.; Blake, C. Adv Protein Chem 1997, 50, 123–159.
51. Surewicz, W. K.; Mantsch, H. H.; Chapman, D. Biochemistry 1993, 32, 389–394.
52. Haris, P. I.; Chapman, D. Biopolymers 1995, 37, 251–263.
53. Jackson, M.; Mantsch, H. H. Crit Rev Biochem Mol Biol 1995, 30, 95–120.
54. Krimm, S.; Bandekar, J. Adv Protein Chem 1986, 38, 181–364.
55. Johnston, N.; Krimm, S. Biopolymers 1971, 10, 2597–2605.
56. Caswell, D. S.; Spiro, T. G. Biochim Biophys Acta 1986, 873, 73–78.
57. Westermark, P.; Li, Z. C.; Westermark, G. T.; Leckstrom, A.; Steiner, D. F. FEBS Lett 1996, 379, 203–206.
58. Kelly, J. W. Nat Struct Biol 2002, 9, 323–325.
59. Nettleton, E. J.; Tito, P.; Sunde, M.; Bouchard, M.; Dobson, C. M.; Robinson, C. V. Biophys J 2000, 79, 1053–1065.
60. Louros, N. N.; Tsiolaki, P. L.; Griffin, M. D.; Howlett, G. J.; Hamodrakas, S. J.; Iconomidou, V. A. Int J Biol Macromol 2015, 79, 711–718.
61. Luk, K. C.; Song, C.; O'Brien, P.; Stieber, A.; Branch, J. R.; Brunden, K. R.; Trojanowski, J. Q.; Lee, V. M. Proc Natl Acad Sci USA 2009, 106, 20051–20056.
62. Liu, C.; Zhao, M.; Jiang, L.; Cheng, P. N.; Park, J.; Sawaya, M. R.; Pensalfini, A.; Gou, D.; Berk, A. J.; Glabe, C. G.; Nowick, J.; Eisenberg, D. Proc Natl Acad Sci USA 2012, 109, 20913–20918.
63. Kuzuya, H.; Blix, P. M.; Horwitz, D. L.; Rubenstein, A. H.; Steiner, D. F.; Faber, O. K.; Binder, C. Diabetes 1978, 27, 184–191.
64. Polonsky, K. S.; Given, B. D.; Van Cauter, E. J Clin Invest 1988, 81, 442–448.
65. Faber, O. K.; Hagen, C.; Binder, C.; Markussen, J.; Naithani, V. K.; Blix, P. M.; Kuzuya, H.; Horwitz, D. L.; Rubenstein, A. H.; Rossing, N. J Clin Invest 1978, 62, 197–203.
66. Louros, N. N.; Iconomidou, V. A.; Giannelou, P.; Hamodrakas, S. J. PLoS One 2013, 8, e73258.
67. Sawaya, M. R.; Sambashivan, S.; Nelson, R.; Ivanova, M. I.; Sievers, S. A.; Apostol, M. I.; Thompson, M. J.; Balbirnie, M.; Wiltzius, J. J.; McFarlane, H. T.; Madsen, A. O.; Riekel, C.; Eisenberg, D. Nature 2007, 447, 453–457.
68. Diaz-Avalos, R.; Long, C.; Fontano, E.; Balbirnie, M.; Grothe, R.; Eisenberg, D.; Caspar, D. L. J Mol Biol 2003, 330, 1165–1175.
69. Nelson, R.; Sawaya, M. R.; Balbirnie, M.; Madsen, A. O.; Riekel, C.; Grothe, R.; Eisenberg, D. Nature 2005, 435, 773–778.
70. Marshall, K. E.; Serpell, L. C. Biochem Soc Trans 2009, 37, 671–676.
71. Nerelius, C.; Alvelius, G.; Jornvall, H. Biochem Biophys Res Commun 2010, 403, 462–467.
72. Hamodrakas, S. J Comput Appl Biosci 1988, 4, 473–477.
73. Kabsch, W.; Sander, C. Proc Natl Acad Sci USA 1984, 81, 1075–1078.
74. McGuffin, L. J.; Bryson, K.; Jones, D. T. Bioinformatics 2000, 16, 404–405.
75. Landreh, M.; Ostberg, L. J.; Jornvall, H. Biochem Biophys Res Commun 2014, 450, 1433–1438.
76. Huang, K.; Dong, J.; Phillips, N. B.; Carey, P. R.; Weiss, M. A. J Biol Chem 2005, 280, 42345–42355.
77. Jimenez, J. L.; Nettleton, E. J.; Bouchard, M.; Robinson, C. V.; Dobson, C. M.; Saibil, H. R. Proc Natl Acad Sci USA 2002, 99, 9196–9201.
78. Brange, J.; Andersen, L.; Laursen, E. D.; Meyn, G.; Rasmussen, E. J Pharm Sci 1997, 86, 517–525.
79. Ghorbani, A.; Shafiee-Nick, R. World J Diabetes 2015, 6, 145–150.
80. Howlett, G. J.; Moore, K. J Curr Opin Lipidol 2006, 17, 541–547.
81. Kaur, G.; Levy, E. Front Mol Neurosci 2012, 5, 79.
82. Mullard, A. Nat Rev Drug Discov 2015, 14, 77–81.
83. Wang, W. Int J Pharm 2005, 289, 1–30.
84. Ludvigsson, J. Front Biosci (Elite Ed) 2013, 5, 214–223.
85. Gupta, Y.; Singla, G.; Singla, R. Indian J Endocrinol Metab 2015, 19, 174–177.
86. Landreh, M.; Johansson, J.; Jornvall, H. Horm Metab Res 2013, 45, 769–773.